

Journal of Organometallic Chemistry, 411 (1991) 239–249
Elsevier Sequoia S.A., Lausanne
JOM 21786

[3]Ferrocenophane bridge reversal barriers

III. Energies of Te_2S , Te_2Se and Te_3 bridged compounds, and a CNDO/2 investigation of the mechanism of the bridge reversal process

Edward W. Abel, Keith G. Orrell, Anthony G. Osborne, Vladimir Šik
Department of Chemistry, The University, Exeter, Devon EX4 4QD (UK)

and Wang Guoxiong

Coordination Chemistry Institute, Nanjing University, Nanjing (People's Republic of China)

(Received January 25th, 1991)

Abstract

Dynamic NMR studies have shown that the energies of the bridge reversal fluxion in the [3]-ferrocenophanes $[\text{Fe}(\text{C}_5\text{H}_4\text{E})_2\text{E}]$ ($\text{E} = \text{S}, \text{Se}, \text{Te}$) are, in terms of ΔG^\ddagger (298 K) data, 56.3, 55.4 and 51.8 kJ mol^{-1} respectively. These values, which are a function of total bridge length, are compared with values for the other trichalcogena-[3]ferrocenophanes. Relative magnitudes of torsional barriers about chalcogen-chalcogen bonds calculated from these data, showed the $\text{Te}-\text{Te}$ torsion energy to be 1.7 kJ mol^{-1} lower than the $\text{Se}-\text{Te}$ torsion and 2.2 kJ mol^{-1} lower than the $\text{S}-\text{Te}$ torsion. The mechanism of the bridge reversal process was investigated by CNDO/2 calculations on $[\text{Fe}(\text{C}_5\text{H}_4\text{E})_2\text{E}]$ ($\text{E} = \text{S}, \text{Se}, \text{Te}$), which showed that a transition state structure involving staggered Cp rings, akin to the half chair conformation of cyclohexane, is considerably more favoured than a structure with eclipsed Cp rings and a planar trichalcogen bridge.

Introduction

Although 1,2,3-trichalcogena-[3]ferrocenophanes have been known for the past twenty years, only recently have syntheses been found for all members of the series. Literature references for synthetic routes to all nine members of the series $[\text{Fe}(\text{C}_5\text{H}_4\text{E})_2\text{E}']$ are as follows: $\text{E} = \text{E}' = \text{S}$ [1], Se [2], Te [3]; $\text{E} = \text{S}, \text{E}' = \text{Se}, \text{Te}$ [2], $\text{E} = \text{Se}, \text{E}' = \text{S}, \text{Te}$ [2] and $\text{E} = \text{Te}, \text{E}' = \text{S}, \text{Se}$ [4]. Such compounds are known to undergo a restricted bridge reversal fluxion analogous to six-membered ring chair-chair conformational exchange. The process can be accurately monitored by dynamic NMR (DNMR) spectroscopy. Previous studies of this type in this laboratory were concerned with the complexes ($\text{E} = \text{E}' = \text{S}, \text{Se}$), ($\text{E} = \text{S}, \text{E}' = \text{Se}, \text{Te}$) and ($\text{E} = \text{Se}, \text{E}' = \text{S}, \text{Te}$) [5]. We now report analogous studies on the missing members of this

series, namely (E = Te, E' = S, Se, Te) complexes. Trends in the magnitudes of their bridge reversal barriers will be discussed in terms of total trichalcogen bridge lengths. Relative torsion energies of like and unlike chalcogen–chalcogen single bonds will be deduced from the NMR data.

The more favoured mechanism for the bridge reversal process has been ascertained by CNDO/2 molecular orbital calculations of the ground state and likely transition state energies of the homochalcogen complexes $[\text{Fe}(\text{C}_5\text{H}_4\text{E})_2\text{E}]$ (E = S, Se, Te).

Experimental

Materials

Samples of the 1,2,3-trichalcogena-[3]ferrocenophanes, $[\text{Fe}(\text{C}_5\text{H}_4\text{E})_2\text{E}]$ (E = S, Se, Te) were kindly donated by Professor Max Herberhold of the University of Bayreuth, Germany.

NMR studies

These were performed on a Bruker AM 250 spectrometer operating at 250.13 MHz for ^1H spectra. A standard B-VT 100 unit was used to control the NMR probe temperature, the calibration of this unit being checked periodically against a Comark digital thermometer. Quoted spectral temperatures are accurate to at least $\pm 1^\circ\text{C}$. NMR bandshape analyses were carried out as previously [5,6] using the authors' version of the DNMR3 program [7]. Spectra of all complexes were recorded on solutions in CDCl_3 .

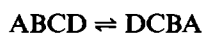
CNDO calculations

Molecular orbital calculations on the ground state and bridge reversal transition state structures of the complexes $[\text{Fe}(\text{C}_5\text{H}_4\text{E})_2\text{E}]$ (E = S, Se, Te) were performed using the CNDO/2 method of Pople et al. [8,9]. Empirical parameters for the various atoms, namely ζ , $(I + A)/2$ and β^0 , were taken from the following sources, atoms, C, H, S [10], Fe [11], Se [12] and Te [13].

Results and discussion

NMR bandshape analyses

The NMR signals of the cyclopentadienyl (Cp) ring protons, when recorded as a function of temperature, are a sensitive monitor of the rate of reversal of the trichalcogen bridge atoms [5]. This process is slow on the ^1H chemical shift time scale at temperatures around -40°C and below. These 'static' spectra consist of four complex signals associated with the four anisochronous protons of each Cp ring (Fig. 1). Each proton has an isochronous but magnetically non-equivalent counterpart in the other Cp ring, but because the static spectra show no evidence of long range couplings between protons on different rings the spin system for the complexes can be accurately described in terms of the spins of a single Cp ring, namely ABCD (Fig. 1). The onset of bridge reversal at higher temperatures will average pairs of protons according to the dynamic spin system:



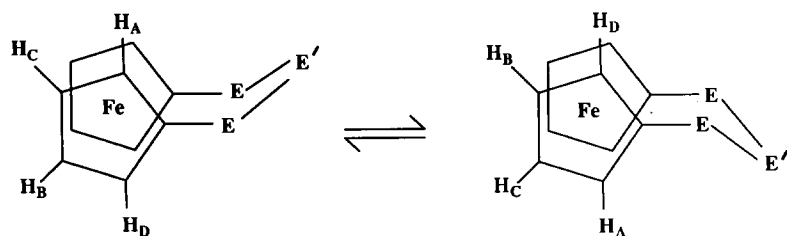


Fig. 1. Static conformers of $[\text{Fe}(\text{C}_5\text{H}_4\text{E})_2\text{E}']$ showing the labelling of ring methine protons.

The chemical shifts and scalar H–H couplings were measured from the ‘static’ spectra of the three complexes and recorded in Tables 1 and 2. The assignments of the four groups of signals to the ring protons A, B, C and D required careful consideration, in view of the variation in absolute and relative chemical shifts of the protons in the three complexes. The identification of mutually exchanging pairs of signals, namely A, D and B, C was achieved by low temperature ^1H saturation transfer experiments on the Te_2S and Te_3 complexes at -30°C and -40°C respectively. The large magnetization transfer effects were clearly due to chemical exchange rather than proton–proton cross-relaxation as they produced negative responses in the ^1H NMR difference spectra. In contrast, NOE effects between protons in small molecules in the extreme narrowing regime are almost always positive [14]. These experiments led to the assignments given in Fig. 2. In the case of the Te_2Se compound the chemical shifts of A and C were so similar that unambiguous assignment of each signal was not possible. Following our previous work [5], proton D was assigned to the lowest frequency signal on the assumption that it experienced the greatest shielding due to the proximity of the axial lone pair of the Te atom. The correct assignment of A and D signals is not essential for the DNMR analysis. However, having made an assignment it is important that the assignment of the other pair of signals, B, C, be internally consistent since different computer simulated spectra would arise from a reversed assignment. This is due to the

Table 1

Hydrogen-1 NMR chemical shifts ^a for $[\text{Fe}(\text{C}_5\text{H}_4\text{Te})_2\text{E}]$ (E = S, Se, Te)

E	T ($^\circ\text{C}$)	ν_{A} (Hz)	ν_{B} (Hz)	ν_{C} (Hz)	ν_{D} (Hz)
S	-30	1135.0	1099.0	1146.0	982.0
Se	-20	1127.5 ^b	1093.0	1130.5 ^b	980.0
Te	-40	1111.0	1088.0	1102.0	999.0

^a At 250.13 MHz relative to Me_4Si (int). ^b Assignments could be interchanged.

Table 2

Spin–spin coupling constants for the ring protons in $[\text{Fe}(\text{C}_5\text{H}_4\text{Te})_2\text{E}]$ (E = S, Se, Te)

E	$^4J_{\text{AB}}$ (Hz)	$^3J_{\text{AC}}$ (Hz)	$^4J_{\text{AD}}$ (Hz)	$^3J_{\text{BC}}$ (Hz)	$^3J_{\text{BD}}$ (Hz)	$^4J_{\text{CD}}$ (Hz)
S	1.25	2.50	1.25	2.50	2.50	1.25
Se	1.26	2.53	1.23	2.44	2.52	1.24
Te	1.25	2.46	1.25	2.39	2.43	1.26

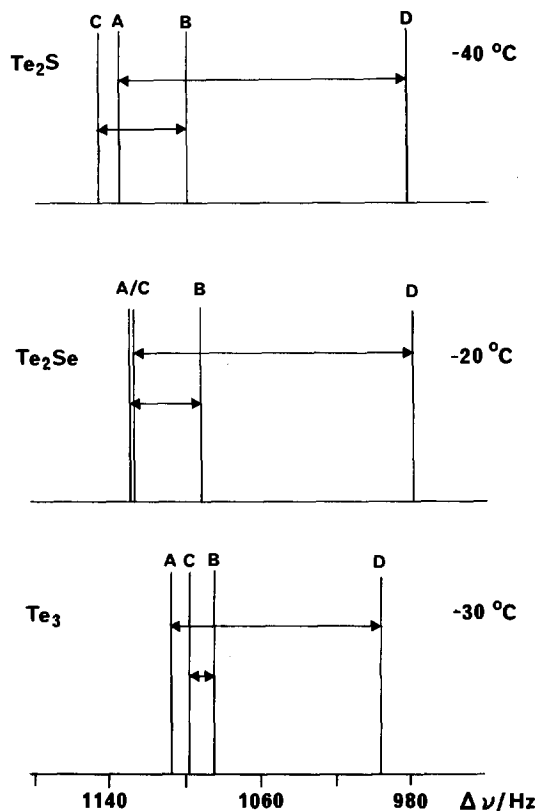


Fig. 2. Schematic diagram of the methine proton chemical shift trends in the series $[\text{Fe}(\text{C}_5\text{H}_4\text{Te})_2\text{E}]$ (E = S, Se, Te).

unequal magnitude of scalar couplings between the two proton pairs, namely ${}^4J_{\text{AB}} \neq {}^3J_{\text{AC}}$ and ${}^3J_{\text{BD}} \neq {}^4J_{\text{CD}}$ (Table 2). The assignments shown in Fig. 2 and Table 2 were the basis of computer simulated dynamic spectra (see later) which very closely matched the experimental spectra, lending further support to their correctness.

There are some notable trends in the Cp ring proton shifts (Fig. 2 and Table 1). On increasing the mass/size of the central bridging chalcogen from S to Se to Te, the chemical shifts of the A, B and C protons all show steady decreases, representing increased shielding. The change in the C proton shift is significantly greater than the others causing the relative chemical shift difference, $(\nu_{\text{C}} - \nu_{\text{A}})$, to change from positive to negative on going from the Te_2S to the Te_3 compound, and being approximately zero for the Te_2Se compound. Both the A and C signals are assigned to ring protons *cis* to the central chalcogen atom (Fig. 1), but it is surprising that the more distant protons, C, are more sensitive to the nature of this chalcogen than the spatially closer A protons.

Having measured the 'static' NMR parameters for the low temperature spectra, variable temperature ${}^1\text{H}$ spectra were recorded in the range -20 to 60°C (-40 to 30°C for the Te_3 complex). The spectra of $[\text{Fe}(\text{C}_5\text{H}_4\text{Te})_2\text{Te}]$ are illustrated in Fig. 3. The highest temperature spectrum consists of two averaged signals due to the rapid bridge reversal process. The lower frequency signal displays some residual exchange

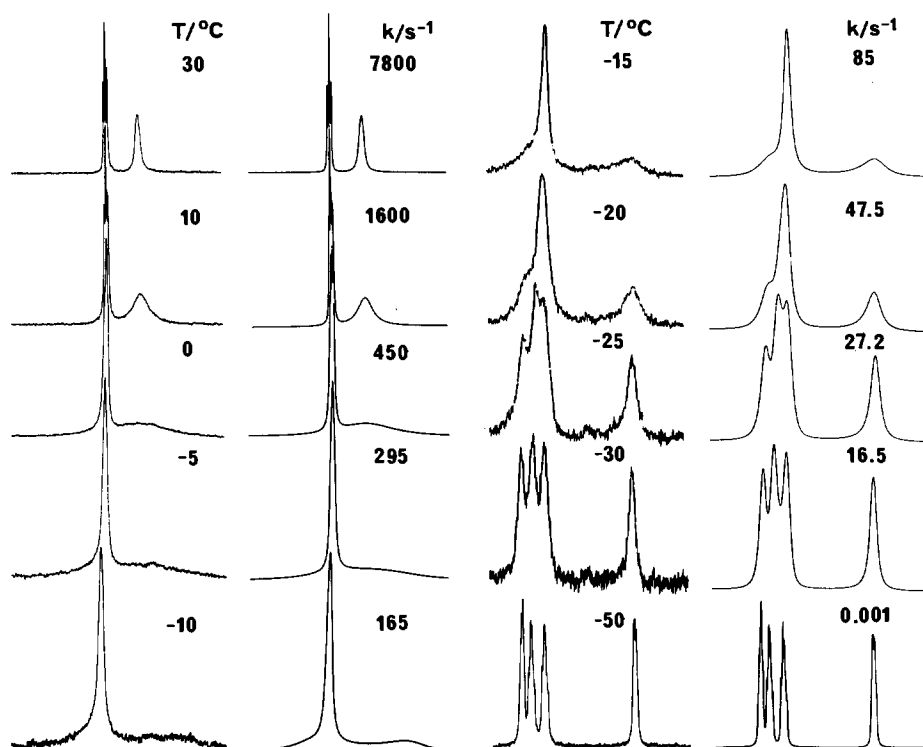


Fig. 3. Variable temperature ^1H NMR spectra of $[\text{Fe}(\text{C}_3\text{H}_4\text{Te})_2\text{Te}]$ in the range -40 to 30°C . Best-fit computer synthesised spectra are shown alongside experimental spectra.

broadening which disappears on elevation of temperature. The intermediate temperature spectra (Fig. 3) exhibit considerable dynamic broadening which could be accounted for by bandshape analyses. Excellent matches were obtained between experimental and computer synthesised spectra. These are shown in Fig. 3 with the optimal rate constant given for each temperature.

The activation parameters for the bridge reversal process in the three complexes are given in Table 3, and compared with the values previously obtained for all the other trichalcogen bridged [3]ferrocenophanes. The new values are all substantially

Table 3

Activation parameters for ring reversal in the complexes $[\text{Fe}(\text{C}_3\text{H}_4\text{E})_2\text{E}']$

E	E'	Bridge length ^a (pm)	ΔG^\ddagger (298 K) (kJ mol ⁻¹)	ΔH^\ddagger (kJ mol ⁻¹)	ΔS^\ddagger (J K ⁻¹ mol ⁻¹)	Ref
S	S	778	80.4 ± 0.2	77.0 ± 0.9	-11.7 ± 2.3	5
S	Se	804	72.6 ± 0.2	69.8 ± 1.1	-9.5 ± 2.9	5
S	Te	844	62.5 ± 0.02	60.5 ± 1.3	-6.8 ± 4.3	5
Se	S	830	71.0 ± 0.1	67.3 ± 0.8	-12.4 ± 2.4	5
Se	Se	856	67.2 ± 0.1	65.8 ± 2.4	-5.0 ± 7.8	5
Se	Te	896	59.9 ± 0.1	57.0 ± 1.1	-9.8 ± 3.5	5
Te	S	910	56.31 ± 0.04	61.9 ± 1.3	18.9 ± 4.5	This work
Te	Se	936	55.35 ± 0.07	63.0 ± 1.4	25.7 ± 4.9	This work
Te	Te	976	51.8 ± 0.2	61.5 ± 1.2	32.5 ± 4.6	This work

^a C-E-E'-E-C length (sum of covalent radii).

lower than the previous ones and exhibit a marked correlation with the total length of the C–Te–E'–Te–C bridge as determined from standard covalent radii. A rather more significant correlation, however, is with the torsional energies of the bonds which constitute this bridge unit. Such a correlation has been shown to be valid for six-membered alicyclic ring reversals [15] and we have shown it to be equally valid in these pseudo-six-membered heterocyclic ring systems [5]. Following the earlier work, it is possible to determine a rough estimate of the relative magnitudes of C–Te and Te–E torsional barriers provided that the contribution to the activation parameter ΔG^\ddagger (or ΔH^\ddagger) from the Cp_2Fe part of the molecule is assumed constant throughout the series.

For example, the bridge reversal energies (as expressed by ΔG^\ddagger values) for $[\text{Fe}(\text{C}_5\text{H}_4\text{Te}_2)\text{S}]$ and $[\text{Fe}(\text{C}_5\text{H}_4\text{S}_2)\text{Te}]$ are 56.3 and 62.5 kJ mol^{-1} respectively. These molecules differ essentially in terms of two C–Te bonds instead of two C–S bonds. Assuming all other contributions to the overall ring reversal energy barrier remain constant, the difference between the two torsional barriers, $V_0(\text{C–S}) - V_0(\text{C–Te})$ may be expressed as $\Delta G^\ddagger(\text{C–S}) - \Delta G^\ddagger(\text{C–Te})$ or $\Delta\Delta G^\ddagger(\text{C–E}) = (62.5 - 56.3)/2 = 3.1 \text{ kJ mol}^{-1}$. This value compares very favourably with the value of 3.9 kJ mol^{-1} derived from far infrared studies of torsional vibrations of $\text{CH}_3\text{–S}$ and $\text{CH}_3\text{–Te}$ bonds in $\text{CH}_3\text{–E–CH}_3$ compounds [16]. Similarly, $V_0(\text{C–Se}) - V_0(\text{C–Te})$ is calculated from the present NMR data to be 2.3 kJ mol^{-1} compared to the directly measured difference of 1.3 kJ mol^{-1} [16].

The magnitudes of torsional barriers about Te–Te bonds compared to other chalcogen–chalcogen bonds may be calculated on the same principles as above. For example, $V_0(\text{S–S}) - V_0(\text{Te–Te})$, may be calculated from ΔG^\ddagger values for $[\text{Fe}(\text{C}_5\text{H}_4\text{S})_2\text{S}]$ (80.4 kJ mol^{-1}) and $[\text{Fe}(\text{C}_5\text{H}_4\text{Te})_2\text{Te}]$ (51.8 kJ mol^{-1}). This energy difference (28.6 kJ mol^{-1}) reflects the difference between $2(\text{C–S}) + 2(\text{S–S})$ barriers of one molecule and $2(\text{C–Te}) + 2(\text{Te–Te})$ barriers of the other. Assuming that the difference between C–S and C–Te torsional barriers is 3.1 kJ mol^{-1} (above) then $V_0(\text{S–S}) - V_0(\text{Te–Te})$ is given by $[(80.4 - 51.8) - (2 \times 3.1)]/2 = 11.2 \text{ kJ mol}^{-1}$. Other relative torsional barriers were obtained in the same way and the full set of values is displayed in Fig. 4.

This method provides relative torsional barrier energies with considerable accuracy but no information on absolute values. Experimental determinations of such values are greatly restricted by difficulties in synthesising suitable compounds, and the only reliable data refer to S–S torsions. Following the previous work, a value of 29 kJ mol^{-1} was chosen as the best value for $V_0(\text{S–S})$ [18,19]. Other absolute values, relative to this base value, are given in Fig. 4, where it will be seen that $V_0(\text{Se–Se})$ is predicted to be 23.2 kJ mol^{-1} and $V_0(\text{Te–Te})$ to be 17.8 kJ mol^{-1} . Unfortunately, there are no experimental data available for direct comparisons. Some *ab initio* MO calculations on MeSSMe and MeSeSeMe [17] provide rather inconclusive data since the trend in barrier energies depended on the choice of basis sets used in the calculations. However, with STO-3G basis sets, the Se–Se torsion was predicted to be lower than the S–S torsion by 6.2 or 5.9 kJ mol^{-1} depending on whether *cis* or *trans* conformations were computed. These values compare favourably with 6.8 kJ mol^{-1} predicted in this present work. Calculated absolute values of $V_0(\text{Se–Se})$ varied from 20.3 to 73.7 kJ mol^{-1} , depending greatly on the choices of basis set and molecular conformation (*cis* or *trans*), and so do not serve as useful direct comparisons.

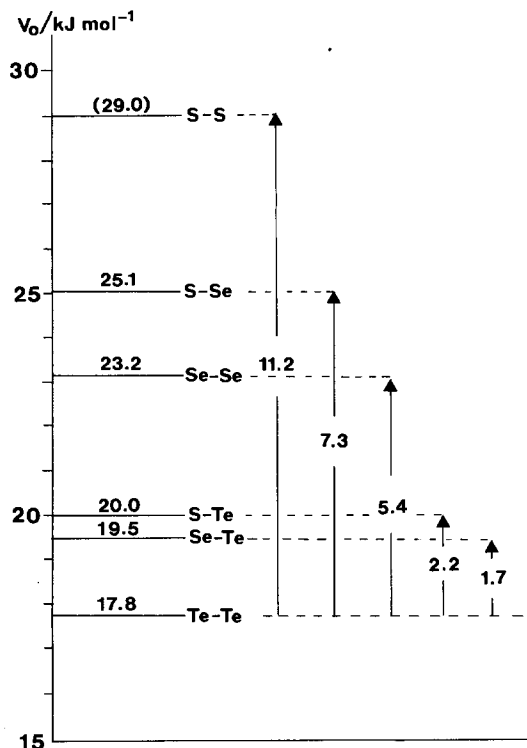


Fig. 4. Absolute and relative torsional energy barriers for [3]ferrocenophane bridge bonds. The value in parentheses for the S-S torsion is based on refs. 18, 19.

We conclude that the present NMR studies combined with the previous studies [5] show quite definitively that the torsional barriers decrease steadily with an increase in mass/size of one or more chalcogens, and, given the reliability of the experimental value of the S-S torsion, all chalcogen-chalcogen torsional energies fall within the range 17.8 to 29.0 kJ mol⁻¹.

Mechanisms of the bridge reversal process

In our earlier studies [5] we followed a previous argument [20] in favouring a mechanism involving rotation about the Cp ··· Fe and chalcogen-chalcogen bridge bonds to produce a conformation with staggered Cp rings rather akin to the half chair conformation of cyclohexane (Fig. 5, structure II). Such an intermediate, or transition state species, was thought likely to be energetically favoured over the intermediate with eclipsed Cp rings and a planar bridge system, (Fig. 5, structure I). In order to seek quantitative evidence for this conclusion CNDO/2 molecular orbital calculations were performed on the ground state and most likely transition state structures of the three homochalcogen complexes [Fe(C₅H₄E)₂E] (E = S, Se, Te).

The geometries of the ground state structures were based on X-ray data [3,21,22] with certain averagings being made in order to allow for the higher symmetry of the rapidly tumbling molecule in solution. The data used for the MO calculations are given in Table 4.

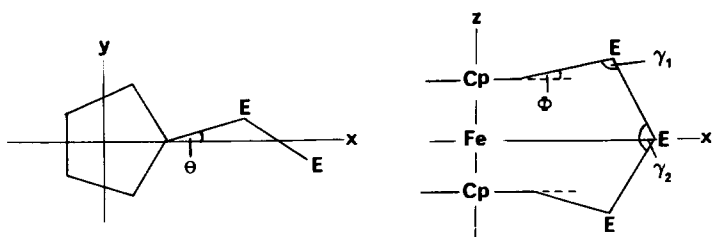
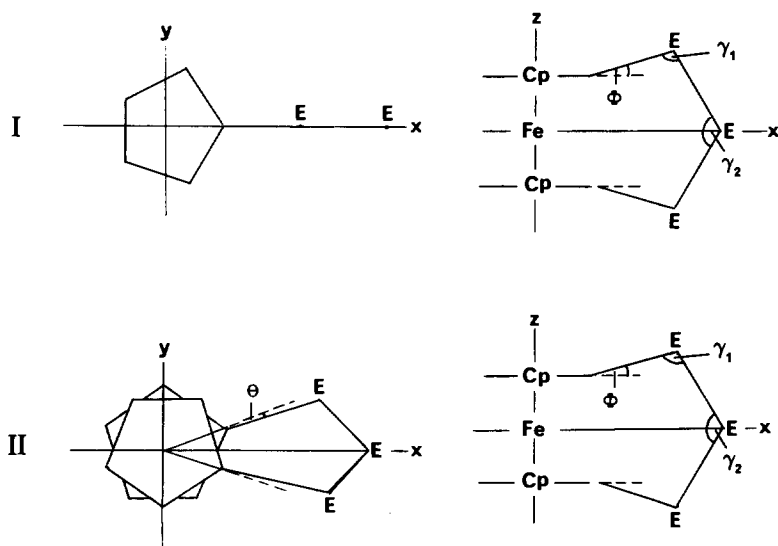
(a) Ground state structure(b) Transition state structures

Fig. 5. Ground state and transition state geometries of $[\text{Fe}(\text{C}_5\text{H}_4\text{E})_2\text{E}]$ which define the angles θ , ϕ , γ_1 and γ_2 .

In $[\text{Fe}(\text{C}_5\text{H}_4\text{S})_2\text{S}]$ the S atoms are almost coplanar with the Cp rings and these rings are mutually parallel. The C-S bonds are not located precisely on the bisectors of the C-C-C angle, the difference between the two C-C-S angles for a given Cp ring being *ca* 3.2° . In the compound $[\text{Fe}(\text{C}_5\text{H}_4\text{Te})_2\text{Te}]$ the two Cp rings are slightly canted to each other, the distance between the ring centres being 3.323 \AA and the C-Te bonds further canted with respect to the rings by *ca* 4.5° in directions away from the Fe atom. This is clearly the result of the larger size of Te atoms compared to S atoms, and the effect will reduce the degree of conjugation of Te with the rings.

The CNDO/2 calculations used the empirical atomic data collected in Table 5. These were carefully chosen from a variety of sources [10-13]. In the calculations of the total molecular energies, E , the angles Cp(plane)-E(ϕ), C-E-E(γ_1), E-E-E(γ_2) and angle θ (all as defined in Fig. 5) were optimised to give minimum energy values while keeping bond lengths constant and preserving appropriate symmetries. These

Table 4

Structural data used for the CNDO/2 calculations of $[\text{Fe}(\text{C}_3\text{H}_4\text{E})_2\text{E}]$ (E = S, Se, Te)

	E = S ^a	E = Se ^b	E = Te ^c
<i>Bond</i> (Å)			
C–Fe	2.0438	2.0438	2.0438
C–C	1.4150	1.4251	1.4351
C–H	0.9825	0.9600	0.9825
C–E	1.7475	1.9259	2.1114
E–E	2.0490	2.3254	2.7566
<i>Angle</i> ^d (°)			
θ	1.6	1.33	3.16
ϕ	0	4.28	7.05
γ_1	102.8	100.15	95.5
γ_2	103.9	100.7	91.6

^a Ref. 21. ^b Ref. 22. ^c Ref. 3 (Structure A). ^d See Fig. 5 for definitions. Values were calculated from the X-ray data.

Table 5

Empirical atomic data used in the CNDO/2 calculations

Atom		ζ	$\frac{1}{2}(I + A)$ (eV)	β° (eV)	Ref.
Fe	4s	1.37	4.12	–23.0	11
	4p	0.425	1.062	–16.0	
	3d	2.722	5.504	–29.0	
Te	5s	2.15	17.35	–11.0	13
	5p	2.15	6.30	–11.0	
Se	4s	2.4394	16.125	–11.0 ^a	12
	4p	2.0718	9.075	–11.0 ^a	
S	3s	1.817	18.5	–29.0	10
	3p	1.817	6.64	–29.0	
C	2s	1.625	12.7	–21.0	10
	2p	1.625	6.10	–21.0	
H	1s	1.20	7.176	–9.0	10

^a Calculations using $\beta^\circ(\text{Se}) = -20$ eV were also performed (See Table 7).

Table 6

Optimised geometries and total electronic energies of the ground state and transition state structures of $[\text{Fe}(\text{C}_3\text{H}_4\text{E})_2\text{E}]$ (E = S, Se, Te)

Bridge	θ	ϕ	γ_1	γ_2	E/E_h	
<i>Ground state structures</i> ^a						
S ₃	1.7	0	106.0	103.9	–134.016316	
Se ₃	1.33	3.0	100.15	–	–130.666385	
Te ₃	0.5	7.05	96.5	91.6	–125.304653	
<i>Transition state structures</i> ^b						
S ₃	I	0.0	3.52	117.33	118.29	–133.982092
	II	5.0	–2.0 ^d	111.29	125.34	–133.988744
Se ₃	I	0.0	9.0	100.15 ^c	113.81	–130.649096
	II	–1.0 ^e	2.0	109.05	117.22	–130.656662
Te ₃	I	0.0	15.0	109.80	110.40	–125.281574
	II	0.0	8.0	109.02	109.88	–125.292294

^a See Fig. 5(a). ^b See Fig. 5(b). ^c Ground state value. ^d C–S bonds canted inwards towards Fe atom.

^e Angle w.r.t. to other side of CCC bisector (Fig. 5(b)).

Table 7

CNDO/2 calculated ring reversal barriers

	ΔE_{I}^a (kJ mol ⁻¹)	ΔE_{II}^b (kJ mol ⁻¹)	$\Delta E(\text{exp})^c$ (kJ mol ⁻¹)
[Fe(C ₅ H ₄ S) ₂ S]	89.87	72.40	80.4
[Fe(C ₅ H ₄ Se) ₂ Se]	68.49 ^d	36.78 ^d	67.2
	45.40 ^e	25.53 ^e	
[Fe(C ₅ H ₄ Te) ₂ Te]	60.61	32.45	51.8

^a Assuming transition state I. ^b Assuming transition state II. ^c NMR-derived values. ^d Using $\beta^\circ(\text{Se}) = -20$ eV. ^e Using $\beta^\circ(\text{Se}) = -11$ eV.

minimum energies corresponding to the optimised geometries of the ground and transition state structures are given in Table 6. Differences between these energies represent the ring reversal barriers. These have been calculated in Table 7 and compared with the NMR-based experimental values. Close quantitative agreement was not expected, given the approximate nature of CNDO calculations and uncertainties in the appropriate values of atomic parameters.

However, agreement is moderately good, particularly for the [Fe(C₅H₄S)₂S] complex. Of rather greater interest, however, are the relative magnitudes of the energy barriers for the two ring reversal mechanisms. In all cases the finding is that the mechanism involving relative Cp ring rotation into a staggered configuration (transition state II, Fig. 5) is much favoured energetically. Thus, the previous assumption [5] that this is the preferred mechanism is now supported by quantitative evidence.

Acknowledgements

We are indebted to Professor Dr. Max Herberhold, (University of Bayreuth, Germany), for supplying the samples of [Fe(C₅H₄E)₂E] (E = S, Se, Te). We thank Dr. Nicholas Long for assistance with the bandshape analyses and useful discussions. This work was supported by NATO research grant RG9/88.

References

- 1 J.J. Bishop, A. Davison, M.L. Katcher, D.W. Lichtenberg, R.E. Merrill and J.C. Smart, *J. Organomet. Chem.*, 27 (1971) 241.
- 2 A.G. Osborne, R.E. Hollands, J.A.K. Howard and R.F. Bryan, *J. Organomet. Chem.*, 205 (1981) 395.
- 3 M. Herberhold, P. Leitner and U. Thewalt, *Z. Naturforsch. B45* (1990) 1503.
- 4 M. Herberhold and P. Leitner, *J. Organomet. Chem.*, 411 (1991) 233.
- 5 E.W. Abel, M. Booth and K.G. Orrell, *J. Organomet. Chem.*, 208 (1981) 213.
- 6 E.W. Abel, M. Booth, C.A. Brown, K.G. Orrell and R.L. Woodford, *J. Organomet. Chem.*, 214 (1981) 93.
- 7 D.A. Kleier and G. Binsch, DNMR3 Program. No. 165, Quantum Chemistry Program Exchange, Indiana University, USA, 1970.
- 8 J.A. Pople, D.P. Santry and G.A. Segal, *J. Chem. Phys.*, 43 (1965) 5129.
- 9 J.A. Pople and D.L. Beveridge, *Approximate Molecular Orbital Theory*, McGraw-Hill, New York, 1970.
- 10 A. Rauk, J.D. Andose, W.G. Frick, R. Tang and K. Mislow, *J. Am. Chem. Soc.*, 93 (1971) 6507.
- 11 A. Serafini, M. Pelissier, J.M. Savariault, P. Cassoux and J.F. Labarre, *Theor. Chim. Acta*, 39 (1975) 229.
- 12 S. Jie and X. Huibi, *J. Mol. Sci. (China)*, 4 (1986) 401.

- 13 L.J. Saethre, N. Martensson, S. Svensson, P.A. Malmquist, U. Gelius and K. Siegbahn, *J. Am. Chem. Soc.*, 102 (1980) 1783.
- 14 H. Kessler, M. Gehrke and C. Griesinger, *Angew. Chem., Int. Ed. Engl.*, 27 (1988) 490.
- 15 J.B. Lambert and S.I. Featherman, *Chem. Rev.*, 75 (1975) 611.
- 16 J.B. Lambert, C.E. Mixan and D.H. Johnson, *J. Am. Chem. Soc.*, 95 (1973) 4634.
- 17 V. Renugopalakrishnan and R. Walter, *J. Am. Chem. Soc.*, 106 (1984) 3413.
- 18 R.R. Fraser, G. Boussard, J.K. Saunders, J.B. Lambert and C.E. Mixan, *J. Am. Chem. Soc.*, 93 (1971) 3822.
- 19 W.N. Hubbard, D.R. Douslin, J.P. McCullough, D.W. Scott, S.S. Todd, J.F. Messerley, I.A. Hossenlopp, A. George and G. Waddington, *J. Am. Chem. Soc.*, 80 (1958) 3547.
- 20 M. Rosenblum, A.K. Banerjee, N. Danieli, R.W. Fish and V. Schlatter, *J. Am. Chem. Soc.*, 85 (1963) 316.
- 21 B.R. Davies and I. Bernal, *J. Cryst. Mol. Struct.*, 2 (1972) 107.
- 22 S.H. Lockhart, M.Sc. Thesis, 1984, University of Virginia, USA (private communication).